Electrostatic Interaction of a Solute with a Continuum. Improved Description of the Cavity and of the Surface Cavity Bound Charge Distribution.

J. L. Pascual-Ahuir and E. Silla

Facultad de Ciencias Quimicas, Universidad de Valencia, Doctor Moliner, 50 BURJASOT (Valencia), Spain

J. Tomasi

Dipartimento di Chimica, Università di Pisa, Via Risorgimento, 35-I 56100 Pisa, Italy

R. Bonaccorsi

Istituto di Chimica Quantistica de Energetica Molecolare (CNR)-Via Risorgimento, 35-I 56100 Pisa, Italy

Received 9 June 1986; accepted 17 November 1986

Algorithms for a finer description of cavities in continuous media and for a more efficient selection of sampling points on the cavity surface are described. Applications to the evaluation of solute surface and volume and to the calculation of the solute-solvent electrostatic interaction energy, as well as of the cavitation energy are shown as examples.

INTRODUCTION

A computational method to introduce solvent effects in the description of molecular systems in the ground state has been proposed by our group few years ago,[1] and later on extended to systems subjected to a change of electronic state.[2] This method has been tested with good results in a fairly large variety of problems (molecular conformations, prototropic equilibria, bimolecular interactions, tautomeric processes, chemical reactions, photochemical processes, etc.).[3–17]

The satisfactory performances of the method prompted us to extend further its range of applicability. As a preliminary step to these extensions, we have considered it convenient to introduce some modifications in the basic computational scheme, giving a better description of some aspects of the solute-solvent interaction without increase of the computational time.

In this note we present a summary of the modifications recently introduced in the algorithm described in Refs. 1 and 2.

Basic outline of the method

The method essentially consists in the introduction of an effective solvent operator $\hat{V}_\sigma$ in the hamiltonian $\hat{H}^\circ_M$ of the solute.

The interaction operator $\hat{V}_\sigma$ is referred to an averaged distribution of the solvent which experiences the influence of M. The derivation of a time-independent Schroedinger equation

$$(\hat{H}^\circ_M + \hat{V}_\sigma)\psi'_M = E'_M\psi'_M \qquad (1)$$

only requires the approximations currently used in quantum mechanics (separation of variables, etc.). $\hat{V}_\sigma$ is then defined in the semiclassical approximation,[11] i.e., limiting the solute-solvent interactions to the classical coulombic and polarization terms, and representing the averaged distribution of the solvent as a continuum. The influence of M on the medium is represented by nonlinear polarization effects.

The method has been amply described elsewhere.[1,2] For the reader's convenience (and

Journal of Computational Chemistry, Vol. 8, No. 6, 778–787 (1987)

CCC 0192-8651/87/060778-10$04.00

upon request of the referees) we summarize here again the main steps.

$\hat{V}_\sigma$ is defined in terms of an apparent charge density $\sigma(\mathbf{s})$ distributed over the surface of a suitable cavity in which the solute M is accommodated. The basic electrostatic relationship

$$\sigma(\mathbf{s}) = -\mathbb{P} \cdot n_\mathbf{s} \tag{2}$$

where n_s is the outer normal to the cavity at position $\mathbf{s}$, may be rewritten in the following way:

$$\sigma(\mathbf{s}) = \frac{\varepsilon - 1}{4\pi\varepsilon} \frac{\partial}{\partial n} (V_\gamma + V_\sigma)_{\mathbf{s}-} \tag{3}$$

where the partial derivative of the potential is computed at a point near $\mathbf{s}$ but immediately inside the cavity. The electrostatic potential is divided into two components, this notation making more evident that there are two physically distinct sources, the total solute charge distribution $\gamma_M(\mathbf{r})$ (electrons and nuclei) and the apparent charge distribution $\sigma(\mathbf{s})$. In addition, $\gamma_M(\mathbf{r})$ also depends on σ, through Eq. (1) (reaction field polarization effects). An iterative solution is employed, although different mathematical approaches to this nonlinear problem are possible.[18]

We begin by defining a zeroth order approximation

$$\sigma^{00}(\mathbf{s}) = \frac{\varepsilon - 1}{4\pi\varepsilon} \frac{\partial}{\partial n} (V\gamma^0)_{\mathbf{s}-} \tag{4}$$

where the notation γ^0 emphasizes the fact that the unperturbed charge distribution of M is employed. σ^{00} is then used to define a provisional value of V_σ, which when introduced in Eq. (3) gives a better description of σ (s), denoted as σ^{01}. After a limited number of cycles (3, as general rule) a final asymptotic value, σ^{0f}, is reached. This value is introduced now in the hamiltonian (1) to get ψ_M^1 and then a partially polarized charge distribution γ_M^1. This new charge distribution γ^1 is introduced in eq. (3) to start a new cycle of refinements of σ, with final value σ^{1f}.

Final self-consistency is reached within three SCF cycles on Eq. (1). The calculations of $\sigma(\mathbf{s})$ are performed for a limited number of $\mathbf{s}$ values, and σ itself is replaced by a finite set of point charges $q_k\delta(\mathbf{r} - \mathbf{s}_k)$ placed at position $\mathbf{s}_k$. These positions define the centers of suitable tesserae on the surface cavity, of area ΔS_k, covering the whole cavity surface

$$q_k = \sigma(\mathbf{s}_k)\Delta S_k \tag{5}$$

The interaction potential is defined accordingly:

$$V_\sigma(\mathbf{r}) = \sum_\mathbf{k} q_k / |\mathbf{r} - \mathbf{s}_M| \tag{6}$$

When the final solution of Eq. (1) is reached, the information encoded in $V_{\sigma'}$, ψ'_M and E'_M can be further elaborated, to get results of different type (solvent effects on solute observables, changes in the free energy, enthalpy and entropy of whole system, etc.) according to the prescription given in the above quoted articles.[1-16] We report here only the expression for the electrostatic contribution to the free energy of the system (i.e., the work of assembling the charges of the M, in solution, at constant temperature and volume), as this quantity is employed in the following section:

$$G = E'_{\text{tot}} - \frac{1}{2} \int \gamma' V_{\sigma'} dr \tag{7}$$

It is convenient to introduce also a solvation free energy (electrostatic part)

$$\Delta G_{\text{el}} = G - E^\circ_{\text{tot}} \tag{8}$$

E'_{tot} and E°_{tot} are the total energies, including also nuclear repulsion, computed at a given geometry of M using, respectively, the solution of Eq. (1) and the solution of the corresponding Schroedinger equation involving $\hat{H}^\circ_M$ only.

To these electrostatic terms, contributions of different origin can be added: terms deriving from limitation of motion of M in the condensed fase, terms related to the difference in the rotational degrees of freedom in gas and in solution, terms related to dispersion effects, terms related to the formation of a cavity in the bulk liquid. We shall consider in the following section only cavitation contributions, which have been computed according to Pierotti's formula,[19] and which depend, to some extent, on the modifications of the computational algorithm we are discussing in this article. Other contributions have been computed and analyzed in other articles.

The solvation free energy with inclusion of cavitation terms take the form

$$\Delta G'_{\text{sol}} = \Delta G_{\text{el}} + G_{\text{cav}} \tag{9}$$

where G_{cav} is a quantity which depends on the volume and surface of the cavity, as well as on other parameters related to the bulk solvent: see refs.[19-20]

The connection with the classical reaction field method[21,22] is evident, but evident also should be the larger potentiality of the present method due to the explicit use of a quantum mechanical formalism.

The explicit definition of the interaction operator in terms of $\sigma(\mathbf{s})$ and its expansion in terms of point charges [Eqs. (5) and (6)] introduce a notable difference with respect to other methods defined in the quantum mechanical formalism and making use of a continuous description of the solvent (for a review see Tapia,[23] and for a more recent proposal, Rivail et al.[24]). In fact, this definition of $\hat{V}_\sigma$ permits a direct representation of the interaction to all the orders, without resorting to truncated multipole expansions, and makes possible the use of cavities of any shape.

These points represent, in our opinion, the main advantages of this computational method. They are preserved in the revised version presented here. The new features of the method introduced here are a different definition of the tesserae on the cavity surface, an improved strategy to adjust the description of the cavity surface and of σ at the intersection of the spheres — when one considers the cavity as an assembly of intersecting spheres centered on the atoms of the solute — and the inclusion of an algorithm to eliminate regions of the outer space too small for accommodating solvent molecules.

The shape of the cavity and the form of the tesserae

Apart from a few test calculations performed over elliptical cavities, all the applications of the method mentioned in the introduction have been conducted using cavities composed of intersecting spheres centered on selected nuclei of M. The tesserae on each sphere were of rectangular shape defined in terms of fixed increments $\Delta\vartheta$ and $\Delta\varphi$ in a local polar reference frame (parallels and meridians as boundaries of the tesserae).

This definition of tesserae presents some defects and is here changed. Reference is made to a solid, the pentakisdodecahedron, $\{3,5+\}_{1,1}$ in the geodesic symbolism,[25] which can be visualized (see Fig. 1) as deriving from the dodecahedron inscribed in the reference sphere, and then defining additional triangles having two vertices in common with those of dodecahedron pentagona and the third vertex on the sphere surface on the perpendicular of the pentagon center. These triangles are the faces of the pentakisdodecahedron (60 in number.)

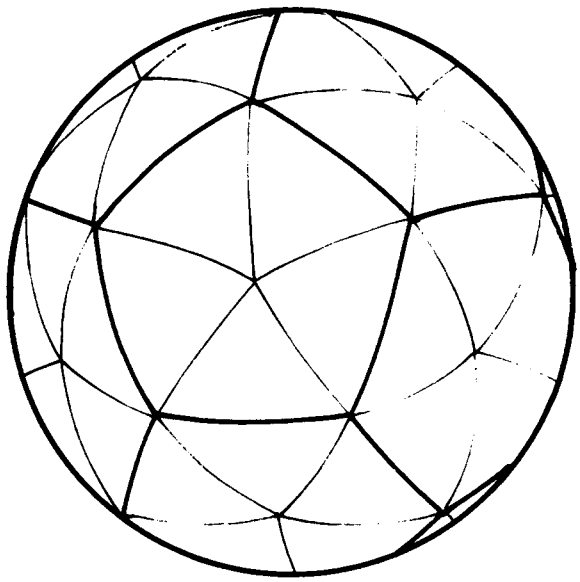

Figure 1. A schematic representation of the tesseral division of a sphere in terms of the pentakisdodecahedron faces. All the vertices of the 60 triangles lie on the sphere.

Each face of the pentakisdodecahedron may be divided in 4 triangles, and so on, defining in this way a sequence of levels of approximations, here numbered $1,2,3\ldots$ where 1 stands for the original pentakisdodecahedron. (The symbols for levels, $2,3\ldots$ in the geodesic symbolism are $\{3,5+\}_{2,2}$, $\{3,5+\}_{4,4},\ldots$)

We recall that in the computational method we require only the coordinates of the centers of the tesserae, and the area of the tesserae. Both data are immediately obtained and stored in the program to avoid superfluous calculations.

These tesserae are more uniform on the surface cavity than the preceding ones and the level of approximation allows the number of points k to be increased with regularity.

More important is the improvement of the description of the surface at the intersection of two spheres.

The new subroutine analyzes whether a triangle (level 1) belonging to the first sphere is completely inside the second sphere or not. In the affirmative, this triangle is eliminated, otherwise a second test checks whether a portion of the triangle is inside the second sphere.

For triangles partly contained in the second sphere a similar analysis is performed at level

2, and so on, until level 5, according to the option given in the input. The results of this procedure are shown in Fig. 2.

The program considers a possible intersection of the sphere K with all the other spheres $L \neq K$ present in the model (see also the next section), using as criteria at level 1 the location of vertices and midpoints of the triangles, at intermediate levels the location of the vertices, at the last level the center only.

When the "external" triangles defining the cavity surface are determined, they are directly employed to compute volume and surface of the cavity (these data are used in the main program as input for the calculation of the cavitation energy, but they are often used in a different way in other physico-chemical models of condensed systems.) The set of charges q_k, defined in Eq. (5) are placed on the center of the triangles of level 1 and on the "mass center" of the set of smaller triangles at higher level. In this way we have for each sphere $k_{max} \leq 60$.

We report in Table I the results for a simple model of an empty cavity, defined as the combination of two spheres with radii $R_1 = R_2 = 2.4$ and distance between the centers $D = 1.54$. The "error" has not a statistical meaning: it indicates the dependence of the results on the orientation of the original dodecahedra with respect to the D axis. The table also gives analogous results obtained with the original definition of tesserae in terms of polar coordinates.

A more complete set of results is presented in Table II. In this case we have considered the HF molecule as solute, in a two-sphere cavity ($R_H = 1.44\, R_F = 1.62\, D_{HF} = 0.92$, values in Å). The calculations of the solvation energy have only an indicative value, having been obtained with a CNDO procedure.

Table II also details the contributions to the surface S due to the two spheres, the value of the electrostatic (ΔG_{el}) and cavitation (G_{cav}) contributions to the solvation free energy, and the computational time in seconds (times refer to a DPS8/52 BULL computer).

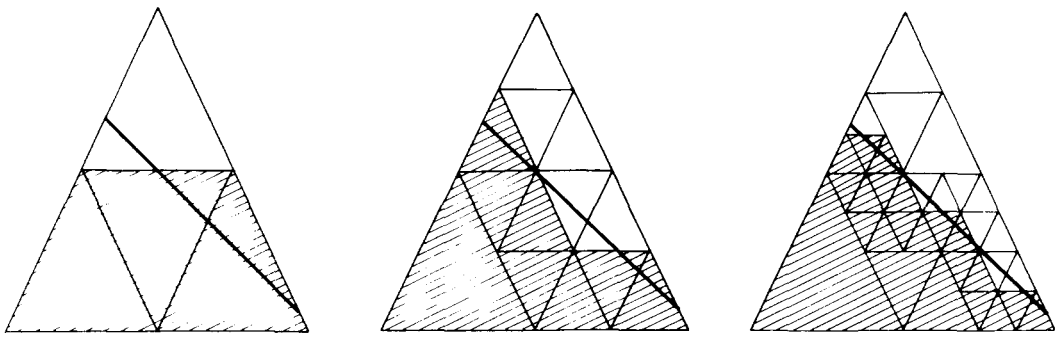

Figure 2. An example of a more precise determination of the cavity surface. The main triangle is one of the 60 faces of the pentakisdodecahedron defined in Figure 1. The solid line is the intersection with a second sphere. At level 2 the contribution on the cavity surface is given by the three shaded triangles. A finer definition is obtained at levels 3, 4 and 5 (the last not shown here).

Table I. Surface (S), volume (V), number of points (points) for a cavity composed by two spheres.

LEVEL	S	V	Points
1	95. ± 3.	84. ± 2.	79 ± 2
2	95. ± 2.	85. ± 1.	86 ± 6
3	94.8 ± 0.6	84.4 ± 0.4	94 ± 5
4	95.5 ± 0.2	85.0 ± 0.1	97 ± 4
5	95.57 ± 0.07	84.98 ± 0.04	97 ± 4
$\Delta\theta = 30\ \Delta\varphi = 36$	101. ± 7.	90. ± 5.	88 ± 8
$\Delta\theta = \Delta\varphi = 25.71$	94. ± 5.	86. ± 2.	134 ± 19
Exact	95.6049	84.8169	

Table II. Surface, volume, number of points, free energy of interaction and of cavitation for HF in a two-spheres cavity.[a]

Level	S	S_F	S_H	V	Points	G_{el}	G_{cav}	Time
1	38.	24.	14.	22.	76	−1.51	4.7	9
	±2.	±2.	±1.	±1.	±5	±0.04	±0.2	±3
2	38.4	23.8	14.5	21.8	87	−1.53	4.78	14
	±0.9	±0.6	±0.4	±0.4	±3	±0.01	±0.09	±1
3	38.79	24.0	14.7	22.06	93	−1.54	4.82	15
	±0.07	±0.1	±0.2	±0.03	±3	±0.00	±0.01	± 2
4	38.69	24.18	14.52	22.03	93	−1.54	4.81	15
	±0.06	±0.07	±0.01	±0.03	±3	±0.00	±0.01	±2
5	38.71	24.22	14.49	22.04	94	−1.53	4.81	16
	±0.02	±0.02	±0.00	±0.01	±2	±0.00	±0.00	±2
$\Delta\theta$ = 30	39.	24.4	14.	21.9	79	−1.52	4.8	11
$\Delta\varphi$ = 36	±1.	±0.4	±1.	±0.4	±8	±0.03	±0.1	±2
$\Delta\theta$ = 25.71	40.	25.	15.	23.	131	−1.58	4.9	29
$\Delta\varphi$ = 25.71	±3.	±2.	±1.	±1.	±6	±0.08	±0.3	±2
Exact	38.7012	24.2188	14.4824	22.0026				

[a] S(Å^2), V(Å^3), G(kcal/mol); time(seconds).

The next example (Table III) is given under the same format. It refers to H_2CO (CNDO calculations, D_{HC} = 1.08 D_{CO} = 1.22 <HCH = 120° R_H = 1.44 R_C = 1.92 R_O = 1.68, distances in Å). The three examples show that in passing from level 1 to level 5 there is a constant improvement of S and V. The corresponding increase of computing time is kept within reasonable limits.

A computationally more complex example is reported in Table IV and Figure 3. It is drawn from an unpublished study on the metabolic activation of the carcinogenic N-nitrosoamines (see Reynolds and Thomson,[26]). The calculations have been done with the 4-21G basis set on a GOULD 32/8705 computer. The computation times are: 16 min. in vacuo, with additional times of 28 min. in solution with the old program (version for Gaussian 70,) and 16 min. in solution with the present program. This example shows how conformational curves may be affected by solvent effects even at the qualitative level, and how the new program reduces computational times without altering the quality of the results. A comparison of numerical estimates of solvation free energy and enthalpy provided by the older version of

Table III. Surface, volume, number of points, free energy of interaction and of cavitation for H_2CO in a five-spheres cavity.[a]

Level	S	S_C	S_O	S_H	V	Points	ΔG_{el}	G_{cav}	Time
1	61.	19.	19.	11.3	42.	109	− 1.23	7.0	22
	±4.	±3.	±2.	±0.5	±2.	±5	±0.03	±0.4	±2
2	62.3	20.1	20.0	11.1	43.0	137	−1.20	7.12	34
	±0.7	±0.3	±0.7	±0.1	±0.4	±5	±0.01	±0.07	±2
3	62.4	19.7	20.36	11.17	42.98	150	−1.19	7.13	41
	±0.1	±0.1	±0.06	±0.06	±0.08	±2	±0.01	±0.01	±1
4	62.3	19.55	20.46	11.17	42.95	154	−1.19	7.12	44
	±0.1	±0.08	±0.04	±0.03	±0.07	±3	±0.01	±0.01	±2
5	62.24	19.49	20.42	11.16	42.89	156	−1.19	7.11	47
	±0.04	±0.05	±0.01	±0.01	±0.03	±3	±0.00	±0.00	±2
$\Delta\theta$ = 30	61.	19.	20.	11.2	42.0	111	−1.21	7.0	23
$\Delta\varphi$ = 36	±2.	±3.	±2.	±0.8	±0.7	±7	±0.05	±0.1	±3
$\Delta\theta$ = 25.71	63.	20.	20.9	10.9	43.	185	−1.20	7.2	59
$\Delta\varphi$ = 25.71	±3.	±2.	±0.7	±0.4	±2.	±9	±0.05	±0.3	±6
Exact	62.2650	19.5122	20.4349	11.1589	42.7599				

[a] S(Å^2), V(Å^3), G(kcal/mol); time(seconds).

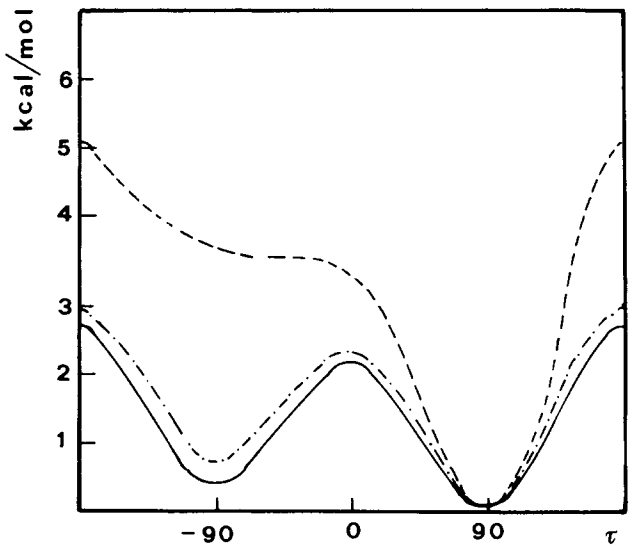

Figure 3. Conformational energy for the rotation of the OH group in $HOCH_2NHNO$. The conformations of this curve are (τ, −90, 180) where the dihedral angles *ABCD* are numbered starting from the left of the formula, with positive angles corresponding to a counterclockwise rotation of the *CD* bond as viewed along the $B \rightarrow C$ direction. Calculations performed with a 4-21G basis set[27], spheres centered on all the atoms (R_H = 1.44, R_C = 1.92, R_N = 1.80, R_0 = 1.68, all values in Å). The starting conformation: all trans. Internal geometry derived from Ref. 27. Full line: in solution, present method; dotted line: in solution, older method; interrupted line: in vacuo. The energies are shifted to a common zero.

Table IV. Surface, volume and energetic values obtained for a set of rotation of the α-hydroxynitrosamine obtained with the older (SPHERES) and new version of the program (POLYHEDRA).[a]

	Old Version (SPHERES)					New Version (POLYHEDRA)			
τ	S	V	$E°$	ΔG_{el}	G_{cav}	S	V	ΔG_{el}	G_{cav}
0	107.37	84.07	3.51	−13.47	11.37	107.13	84.91	−13.23	11.35
90	108.55	85.12	0.00	−12.26	11.48	106.56	85.84	−11.91	11.30
180	109.36	85.03	5.09	−14.36	11.56	107.83	84.96	−14.34	11.42
270	109.09	85.08	3.84	−15.42	11.53	107.96	85.15	−15.39	11.43

[a]The conformations and the computational details are reported in the caption of Figure 3. Dihedral angles in degrees; S in Å^2; V in Å^3; $E°$ (conformation energy in vacuo), ΔG_{el} (solvation free energy), G_{cav} (cavitation energy) in kcal/mol.

the method with those derived from other sources (experiment and calculation) may be found in Refs. 9 and 17.

These examples, to us, seem sufficient to demonstrate the superiority of the present method with respect to the preceding one, considering both precision and computational time.

Identification of solvent excluded volumes

A cavity defined in terms of spheres centered on solute atoms eliminates for asymmetric solutes the defect of older methods, which where obliged to include in the cavity a portion of space actually occupied by the solvent. Cavities of this kind (corresponding to the envelope of Van de Waals surfaces) are, in fact, often employed in pictorial representations of the solute. A minor defect for the continuum representation of the solvent is due to the fact that they may define as external to the cavity some limited regions of space where in reality a solvent molecule of finite size cannot penetrate. A pictorial example is given in Figure 4.

A device to eliminate these artifacts is done by the well known method of the rolling sphere[28]. This method is not convenient in our case because the calculation of the reference points $\mathbf{s}_k$ [see Eq. (5)] is time consuming, and

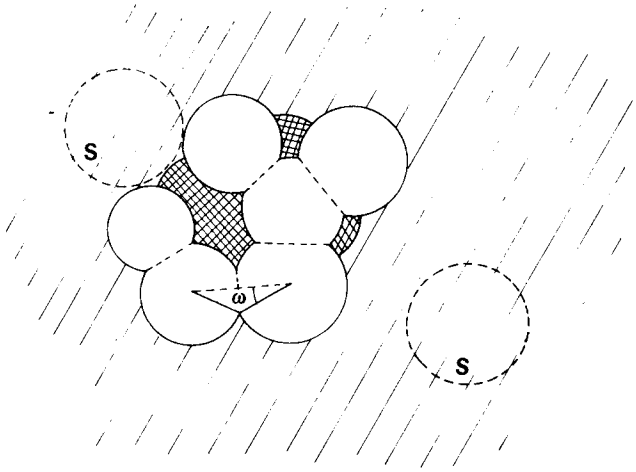

Figure 4. An example of the determination of the outer excluded volume (for a solvent of radius R_s). The white area represents the original cavity and the crossed area the cavity enlargement due to the excluded volume.

because the evaluation of the reaction potential is considerably simpler if the surface is at every point locally convex.

In the program described here we eliminate these portions of the outer space by adding extra spheres, automatically defined by the program.

The process of creation of new spheres is activated by a test involving the distance D_{KL} between the centers of all the couples of spheres K,L already present. A couple is eligible for creation of new spheres if

$$D_{KL} < (R_K + R_L + 2R_S) \qquad (10)$$

where R_S is the radius of the solvent molecule, considered here as a rigid sphere. A limitation in the number of new spheres is provided by additional tests involving: (a) the reciprocal visibility of K and L, (b) the amount of overlap between K and L, and (c) the radius of the new sphere.

Reciprocal Visibility

If there is a third sphere M eclipsing L with respect to K, the K-L couple is no more considered as a possible source of new spheres. M eclipses the KL couple if

$$D_{M,KL} < f \cdot R_M \qquad (11)$$

where $D_{M,KL}$ is the distance of the center of M with respect to the K-L axis. The numerical factor f can be freely selected in the input ($0 < f < 1$) in order to allow a greater flexibility in the creation of new spheres. The value $f = 0.5$ has been selected for normal runs.

Amount of Overlap

If there is partial overlapping of the two spheres ($D_{KL} < R_K + R_L$) a second limiting condition is desiderable. In fact, if there is a large overlap, the solvent-excluded outer space is small and the additional spheres should be small and with little practical effect. The overlapping is measured in terms of the ω angle giving D_{KL} in function of R_K and R_L

$$D_{KL} = R_K \cos \omega + \sqrt{R_L^2 - R_k^2 \operatorname{sen}^2 \omega} \qquad (R_K < R_L) \qquad (12)$$

After some tests we have selected $\omega \leq 50°$ as threshold for the correction, this value seeming to us a reasonable compromise between precision and number of spheres.

Minimal Radius of the Spheres

The addition of new spheres having a too small radius encumbers the computation without producing significant improvements in the results. The introduction of a minimal radius is thus advisable. Moreover, the process of definition of new spheres is done in an iterative way, because we consider it convenient to repeat the cycle of tests over the K-L couples including also the new spheres: the introduction of a minimal radius is a sensible way to stop this iterative process. We have selected $R_{\min} = 0.2$ Å, i.e., the largest value for a sphere surrounded by 3 rigid tangent spheres corresponding to H_2O molecules.

The definition of the new spheres

Two general cases have been considered. The discrimination between the two cases is given by the difference

$$D_{KL} - \{[(R_K + R_S)^2 - (R_S + R_{min})^2]^{1/2} + [(R_L + R_S)^2 - (R_S + R_{min})^2]^{1/2}\} \quad (13)$$

A negative, or zero, value brings to the definition of a new sphere (A) centered on the K-L axis at the point equidistant from the K and L surfaces and tangent to S.

A positive value of Eq. (7) brings to the definition of a new sphere (A) centered at the point of intersection of the K-L axis with the L surface ($R_L > R_K$) and tangent to S: in the case of $R_K = R_L$ two spheres are added.

The algorithm briefly described here is computationally simple and sufficient for all the cases we have tested. A pictorial example of the obtainable results is done in the already reported Figure 4.

An interesting test is given by the progressive separation of a bimolecular system KL. Figure 5 gives the results for an actual case. The maximum number of additional spheres is 3 (near D_{KL} = 6.5 Å). The two additional spheres at D_{KL} = 7.5 Å are just discarded because $R_A < R_{min}$.

The data of Table IV and Figures 6 and 7 refer to an example drawn from an unpublished study of the conformational properties of normal alcohols (calculations with the STO-3G basis set performed on a GOULD 32/8705 computer). In Figure 6 we report the values of ΔG_{el} [Eq. (8)] obtained without and with the inclusion of additional spheres for a set of related conformation of n-octanol. The shape of n-octanol in the present set of conformations is still compact, see Figure 7, but in compounds with longer chains the effect of excluded volume may be dramatic.

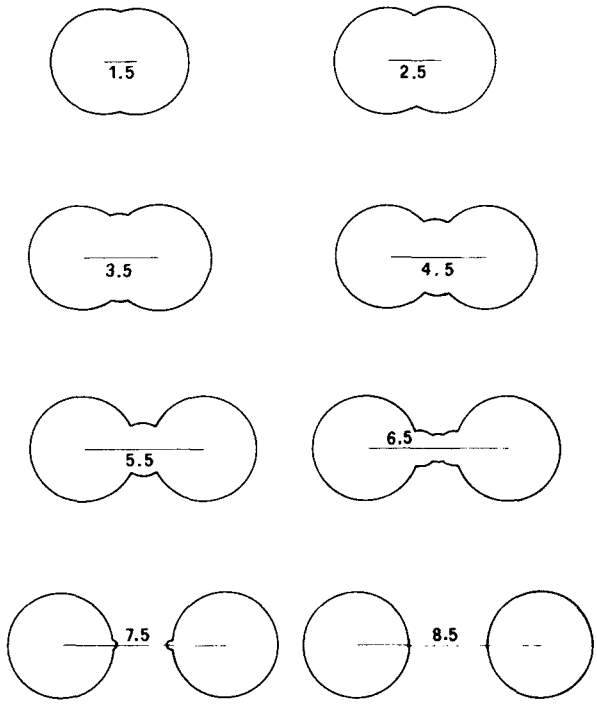

Figure 5. An example of cavities considering also the excluded volume for the dissociation of a biatomic molecule KL. $R_K = R_L = 2.4$.

Conclusions

The modifications to the description of the cavity and of the sampling points on the cavity surface we have documented here is a remarkable improvement of the earlier method employed in the electrostatic model of Ref. 1. The availability of realistic and flexible models for cavities and sampling points is of interest also for other applications in the domain of solutions. We have already mentioned the interest to know the solvent-exposed surface of the solute, and the volume of the solute, for which other methods at different levels of precision are available:[29,30] a different technique, especially when coupled to procedures able to compute at the same time interaction terms,

Table V. Surface, volume, and energetic values obtained with the new program, with and without the inclusion of additional spheres.[a]

	With Additional Spheres					Without Additional Spheres			
τ	S	V	E°	ΔG_{el}	G_{cav}	S	V	ΔG_{el}	G_{cav}
0	172.69	162.65	58.24	−13.23	17.37	173.47	161.63	−13.56	17.44
60	180.06	166.53	2.36	−13.18	18.04	181.49	165.76	−13.84	18.17
120	182.13	166.96	3.70	−13.08	18.23	183.35	166.12	−13.43	18.34
180	182.59	168.05	0.00	−12.51	18.27	183.56	166.50	−13.37	18.35
240	173.73	165.81	20.40	−12.72	17.46	176.54	164.78	−12.98	17.72
300	166.31	159.34	147.07	−12.23	16.79	166.99	159.09	−12.50	16.85

[a]Dihedral angles in degrees; S in Å^2; V in Å^3; E° (conformation energy in vacuo), ΔG_{el} (solvation free energy), G_{cav} (cavitation energy) in kcal/mol.

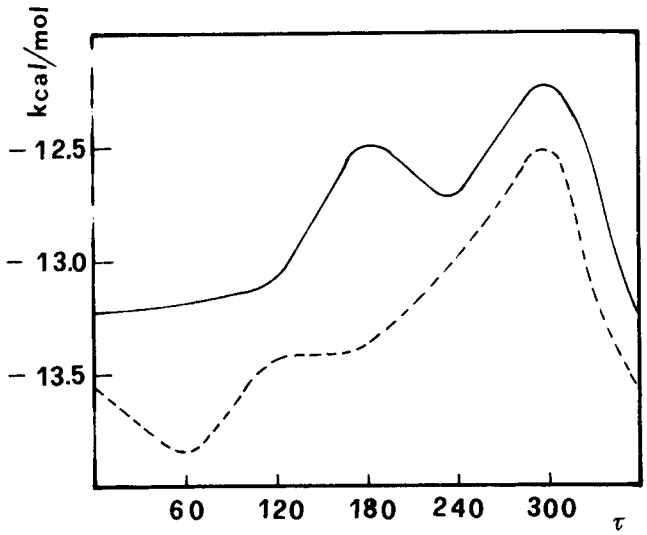

Figure 6. Solvation free energies (ΔG_{el}) for a set of conformations of CH_3-CH_2-CH_2-CH_2-CH_2-CH_2-CH_2-CH_2-OH. The conformations is (0, −90, 90, τ, −60, 0, 150) (same notation as in Fig. 3). Calculations performed with a STO-3G basis set, standard internal geometry and cavity spheres centered on the CH_3, CH_2, O, and H centers (van der Waals radii). Full lines: present method with the inclusion of new spheres; interrupted lines: present method without the inclusion of new spheres.

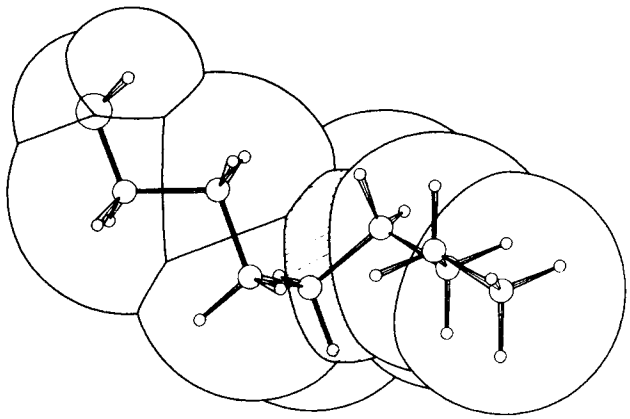

Figure 7. A pictorial view of one of the conformations of n-octanol considered in Table V and Figure 6. The additional spheres are shaded.

should find useful applications. Other applications are more related to the general technique of introducing effective operators in the solute hamiltonian via a continuous distribution of the solvent (not necessarily homogeneous), and a cavity surface representation, limited until now to the coulombic plus polarization effects. Among these applications we quote the evaluation of the dispersion energy, and of the effect of heavy atoms in the solvent on the solute properties, both of which are at present under examination.

References

1. S. Miertus, E. Scrocco, and J. Tomasi, *Chem. Phys.*, **55,** 117 (1981).
2. R. Bonaccorsi, R. Cimiraglia, and J. Tomasi, *J. Comp. Chem.*, **4,** 567 (1983).
3. R. Bonaccorsi, C. Ghio, and J. Tomasi, *Studies in Physics and Theoretic Chemistry,* R. Carbò, ed., Elsevier, 1982, Vol. 21, pag. 407.
4. S. Miertus and J. Tomasi, *Chem. Phys.*, **65,** 239 (1982).
5. A. Duben and S. Miertus, *Chem. Phys. Letters,* **88,** 395 (1982).
6. R. Cimiraglia, S. Miertus, and J. Tomasi, *Chem. Phys. Letters,* **80,** 286 (1981).
7. R. Bonaccorsi, R. Cimiraglia, S. Miertus, and J. Tomasi, *J. Mol. Struct.* (Theochem), **94,** 11 (1983).
8. R. Bonaccorsi, R. Cimiraglia, and J. Tomasi, *Chem. Phys. Letters,* **99,** 77 (1983).
9. R. Bonaccorsi, R. Cimiraglia, P. Palla, and J. Tomasi, *J. Am. Chem. Soc.*, **106,** 1945 (1984).
10. R. Bonaccorsi, R. Cimiraglia, and J. Tomasi, *J. Mol. Struct.* (Theochem), **107,** 197 (1984).
11. R. Bonaccorsi, C. Ghio, and J. Tomasi, *Int. J. Quant. Chem.*, **26,** 637 (1984).
12. M. Persico and J. Tomasi, *Croat. Chem. Acta,* **57,** 1395 (1984).
13. G. Alagona, R. Bonaccorsi, C. Ghio, and J. Tomasi, *J. Mol. Struct.* (Theochem), **135,** 39 (1986).
14. G. Alagona, R. Bonaccorsi, C. Ghio, and J. Tomasi, *J. Mol. Struct.* (Theochem), **137,** 263 (1986).
15. R. Bonaccorsi, E. Scrocco, and J. Tomasi, *Int. J. Quant. Chem.*, **29,** 717 (1986).
16. O. Ventura, A. Lledos, J. Bertran, R. Bonaccorsi, and J. Tomasi, to be published.
17. R. Bonaccorsi, E. Scrocco, and J. Tomasi, *J. Biosc.*, **8,** 627 (1985).

18. J. E. Sanhueza, O. Tapia, W. J. Laidlaw, and M. Trsic, *J. Chem. Phys.*, **70,** 3096 (1979).
19. R. A. Pierotti, *Chem. Rev.*, **76,** 717 (1976).
20. M. H. Abraham and A. Nasehdazeh, *J. Chem. Soc. Faraday Trans.*, **77,** 321 (1981).
21. J. E. Kirkwood, *J. Chem. Phys.*, **2,** 351 (1934).
22. L. Onsager, *J. Am. Chem. Soc.*, **58,** 1486 (1936).
23. O. Tapia in *Molecular Interactions Vol. 3,* H. Ratajczak and W. J. Orwille-Thomas, Eds., Wiley, New York, 1982, pag. 47.
24. J. L. Rivail, B. Terryn, D. Rinaldi, and M. F. Luiz-Lopez, *J. Mol. Struct.* (Theochem), **120,** 387 (1985).
25. H. S. M. Coexter, *Regular Complex Polytopes,* Cambridge University Press, Cambridge, England, 1974.
26. C. A. Reynolds and C. Thomson, *J. Chem. Soc.,* Perkins II, to be published.
27. P. Pulay, G. Fogarasi, F. Pary, and J. E. Boggs, *J. Am. Chem. Soc.*, **101,** 2550 (1979).
28. R. B. Hermann, *J. Phys. Chem.*, **76,** 2754 (1972).
29. B. K. Lee and F. M. Richards, *J. Mol. Biol.*, **55,** 379 (1971).
30. M. H. Zehfus, J. P. Seltzer, and G. D. Rose, *Biopolymers,* **24,** 2511 (1985).